Microspheres viscous drag at a deformed fluid interface: particle's weight and electrical charges effects

Nadia Ben'Mbarek, Adel Aschi, Christophe Blanc, Maurizio Nobili

Microspheres viscous drag at a deformed fluid interface: particle's weight and electrical charges effects

Nadia Ben 'MBarek and Adel Aschi
Université de Tunis El Manar, Faculté des Sciences de Tunis,
LR99ES16 Laboratoire Physique de la Matière Molle et de la Modélisation Électromagnétique, 2092 Tunis, Tunisia

Christophe Blanc and Maurizio Nobili
Laboratoire Charles Coulomb (L2C), UMR 5221 CNRS-Université de Montpellier, Montpellier, France
(Dated: February 4, 2021)

When a microparticle is trapped at a fluid interface, particle's electrical charge and weight combine to deform the interface. Such deformation is expected to affect the particle diffusion via hydrodynamics boundary conditions. Using available models of particle induced electrostatic deformation of the interface and particle dynamics at the interface, we are able to analytically predict particle diffusion coefficient values in a large range of particle's contact angle and size. This might offer a solid background of numerical values to compare with for future experimental studies in the field of particle diffusion at a fluid interfaces.

PACS numbers:

Introduction

The physics of the particles trapped at an interface between two fluids has gained much interest in recent years [1–8]. Novel systems such as Pickering emulsion and BIJEL (Bicontinous Interfacially Jammed Emulsion) consisting in emulsions and gels stabilized by colloidal particles emerged as potential candidates for new functional materials [9, 10]. In these systems, colloidal particles are strongly adsorbed at the interface between two immiscible fluids owed to a decrease of the interfacial energy. Crucial parameters affecting the properties of the final material are the contact angle of the adsorbed particles, their interactions and their related dynamics at the interface.

Direct and inverse oil-in-water emulsions can be formed, in general, by properly controlling the surface properties of the particles and the choice of the fluids. Contact angles in the range 30°-90° favor oil-in-water emulsions, whereas values in the range of 90°-110° lead to water-in-oil emulsions [11].

Interactions between particles at the interface affect also the stability of these particles laden interfaces. Electrostatic repulsions between charged particles in conjugation with the finite area of the droplets are often sufficient to stabilize emulsions [12]. Besides repulsive interactions, attractive interactions can also play an important role. This is the case for larged-size (tens of microns) particles for which gravity cannot be neglected. Under the effect of the particle weight, the interface locally deforms giving rise, when two of such deformations overlap, to an attractive force [13],[14]. Independently from the particle weight a similar attractive force may also arise for smaller charged particles as measured by Nikolidais et al. for $PMMA$ particles at an oil-water interface [15]. In order to explain the presence of such attraction these authors speculated on the presence of an interface deformation generated by the electrostatic stress associated to the particle electric charge. Due to different dielectric constants of the two fluids at the interface an electrical dipole is indeed built up at the particles positions. The dipole electric field generates a non-homogeneous electrostatic pressure on the interface inducing its deformation in the so called *electrodipping effect*. These results stimulated further theoretical researches in order to properly model such an effect. Oettel et al.[16],[17], minimizing the complete free energy of the problem, were able to find an analytical solution of the interface profile and of the interaction between a particle pair in the limit of small amplitude deformations.

On the other hand, dynamics of particles at a fluid interface reveals to be particularly important in the case of kinetically arrested structures as in BIJEL [18]. The viscous drag of a particle depends on the contact angle in the general case of fluids with different viscosities [19, 20] and on the dynamics of the triple line where the three phases meet together [21]. Local interface deformations may also give a noticeable contribution to the particle drag as suggested by Danov et al [22]. In bulk, the viscous drag coefficient at low Reynolds number is governed by the Stokes law: $\Gamma_B = 6\pi\eta R$, where η is the dynamical viscosity of the fluid and R is the radius of the particle. The presence of an interface between two fluids changes the boundary conditions of the particle induced flow and in general affects the particle's viscous drag. In the case of an air-water interface, the particle drag $\Gamma_S$has to depend on the partition of the particle between the fluids. Such partition is governed by the particle contact angle θ at the interface given by local equilibrium condition between the three surface tensions γ_{PW} (Particle-Water), γ_{PA} (Particle-Air) and γ (air-water) via the Young relationship: $\cos\theta = (\gamma_{PW} - \gamma_{PA})/\gamma$.

Danov et al [22] were the first to treat the dependence of the viscous drag versus the contact angle. They predict a

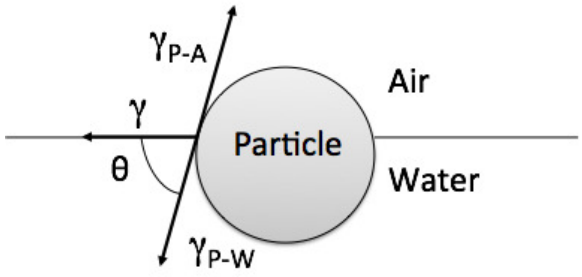

FIG. 1: Particle contact angle θ resulting from the local equilibrium of surface tension at the triple line.

decrease of the viscous drag with the increasing of the contact angle, i.e. when the particle increases its protrusion in air. Later on, Pozirikidis [20] refined the model by considering the small interface deformation induced by the particle motion. In fact due to the particle movement, the water pressure in front (beyond) of the particle is larger (lower) than the one far away from the particle due to the liquid resistance to the particle motion. Such pressure difference is much smaller and at the first approximation null in air. The pressure difference between water and air acts like a Laplace pressure on the interface inducing its deformation. Numerical calculations allow taking into account such effect for the particle drag. Unfortunately, predictions of this model concern very few contact angles making difficult the comparison with experiments. More recently Fisher et al. [19] published a model able to give the viscous drag coefficient for all possible contact angles. The interface considered in this model is flat and incompressible. This last condition corresponds to an interface weakly contaminated and gives a supplementary constraint to the flow which explains the lower diffusion coefficient predicted by the Fischer model with respect to the Pozirikidis one. Note that in all these models the particle viscous drag scales linearly with the particle size resulting in a ratio of drag coefficients at the interface and in the bulk Γ_S/Γ_B independent from the particle radius R.

In this paper we discuss the effects of the interface deformation on the viscous dynamics of a microsphere trapped at an initially flat interface. The deformations considered in this work are the ones induced by the presence of the particle itself via its weight and electrical charges. Dependence of viscous drag ratio over particle size is expected when one considers electrodipping and gravity effects on the particle and on the interface nearby the particle. In order to evaluate such effects on a spherical particle having an uniform surface charge distribution σ_e, we consider the approaches of Oettel et al. [16] and Foret et al. [23].

In the situation of zero gravity and electrostatic effects, the bead sits (see Figure 2(a)) at the air-water interface with a contact angle θ given by the Young relationship and it occupies a circular section of the interface of radius $r_{0ref} = R\sin\theta$. In the limit of weak forces on the particle with respect to the capillary force, the particle slightly sinks in water and weakly deforms the interface (see Figure2 (b)). As a consequence the triple line moves toward the top of the particle in air and the air-water interface sinks until reaching a depth h with respect to this elevation far from the particle. From Figure 2(b), an effective contact θ_{eff} angle can be defined as the angle between the flat interface far from the particle and the tangent to the particle at the extrapolation point. In a first approximation we expect that θ_{eff} will govern the dynamical behavior of the particle.

The effective contact angle θ_{eff} is related to the angle β (see Figure 2(b)) by :

$$\theta_{eff} = \arccos\left(\frac{h}{R} + \sin\beta\right), \tag{1}$$

where the angle β is given by:

$$\beta = \arctan\left(\frac{-1 + \sqrt{1 + 4\epsilon_F(-\epsilon_F + \cot\theta)}}{2\epsilon_F}\right), \tag{2}$$

with ϵ_F given by:

$$\epsilon_F = -\frac{F}{2\pi\gamma r_{0ref}}, \tag{3}$$

where F is the total bulk force acting on the bead. The parameter ϵ_F represents the ratio between the total force F and the capillary force on the bead. In the same way, we can also define the ratio between the total force on the interface and the capillary one as:

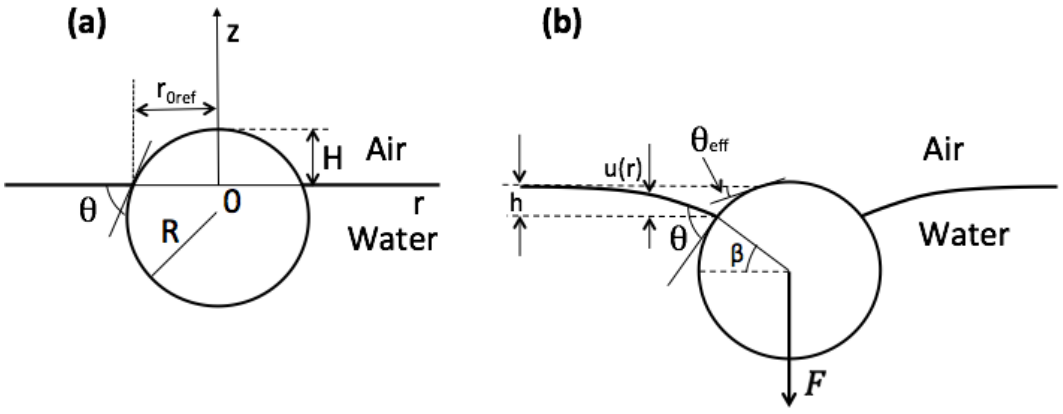

FIG. 2: (a) Reference configuration of a bead with contact angle θ at the flat water-air interface. (b) Under gravity force, electrostatic and osmotic pressures, the reference configuration is perturbed. Local equilibrium at the triple line provokes a displacement of the triple line toward the top of the bead in air, an immersion of the bead in water and a deformation of the interface.

$$\varepsilon_{\wp} = \frac{1}{\gamma r_{0ref}} \int_{r_{0ref}}^{\infty} dr r \wp(r), \tag{4}$$

where $\wp(r)$ is the pressure acting on the interface. In the limit of small perturbations $\epsilon_F, \epsilon_{\wp} \ll 1$, the angle θ_{eff} writes:

$$\theta_{eff} \approx \theta - \left(\frac{h}{r_{0ref}} + \epsilon_F \right), \tag{5}$$

In order to compute θ_{eff} one needs to know the deformation amplitude h and the force acting on the bead F. To access to these parameters Oettel et al. [16] considered all the energy contributions to the problem, and minimized the total free energy of the system in the limit $\epsilon_F, \epsilon_{\wp} \ll 1$. The interface profile $u(r)$ then results in :

$$u(r) = \frac{1}{\gamma} I_0(r/\ell_C) \int_r^{\infty} s\wp(s) K_0(s/\ell_C) ds + \frac{K_0(r/\ell_C)}{\gamma} \left[A + \int_{r_{0ref}}^{r} s\wp(s) I_0(s/\ell_C) ds \right], \tag{6}$$

where K_0 and I_0 are modified Bessel functions of zero order, $\ell_C = \sqrt{\gamma/\rho_w g}$ is the capillary length (ρ_w is the water density and g the gravitational acceleration) and A is a constant obtained by imposing the local equilibrium of forces at the triple line:

$$A = -\frac{\gamma \ell_C \epsilon_F}{K_1(r_{0ref}/\ell_C)} + \frac{I_1(r_{0ref}/\ell_C)}{K_1(r_{0ref}/\ell_C)} \int_{r_{0ref}}^{\infty} s\wp(s) K_0(s/\ell_C) ds. \tag{7}$$

The deformation amplitude $h = -u(r = r_{0ref})$ writes:

$$h = -\frac{I_0(r_{0ref}/\ell_C)}{\gamma} \int_{r_{0ref}}^{\infty} s\wp(s) K_0(s/\ell_C) ds - \frac{A}{\ell_C}, \tag{8}$$

The force acting on the bead F has two contributions: one from gravity F_g and one from the electrostatic F_{el} due to the coupling of the electrical charges on the particle and the local electric field at the interface. The gravity force writes:

$$F_g = -\frac{4\pi R^3}{3} \rho_p f(\theta), \tag{9}$$

where $f(\theta) = 1 - \rho_w/2\rho_p - 3\rho_w/4\rho_p \cos\theta + \rho_w/4\rho_p \cos^3\theta$ takes into account the dependence of the particle's buoyancy on its immersion depth, ρ_p is the particle's density. In order to find an expression of the electrical force on the bead one has to realize that such a force is an internal force to the system. The electrical force on the bead is the opposite of the one acting on the interface:

$$F_{el} = -2\pi \int_{r_{0ref}}^{\infty} r\wp(r)dr. \tag{10}$$

Both the force and the interface deformation depend on the pressure $\wp(r)$ acting on the interface which comes from the osmotic pressure of counter-ions and from the electrostatic pressure related to local electric fields. Both pressures tend to push the interface toward the air side. Considering air and water as two dielectrics and in the limit of Debye-Huckel approximation, Foret et al. [23], found $\wp(r)$ as:

$$\wp(r) = \frac{1}{2}(\varepsilon_w k \varphi_{el}(r,0))^2, \tag{11}$$

where ε_w is the dielectric constant of water, $k = \sqrt{2n_s e^2/\varepsilon_w K_B T}$ is the inverse of the Debye screening length (n_s number density of ions, e the electron electrical charge) and $\varphi_{el}(r,z)$ is the electrostatic potential. In order to calculate $\varphi_{el}(r,z)$, Foret et al. solve the Poisson-Boltzmann equation in the Debye-Huckel approximation for a point charge Q fixed at the center of the interface section occupied by the particle. The asymptotic expression of the potential (valid for $r \gg R, k^{-1}$) writes:

$$\varphi_{el}(r,z) = \frac{Q}{2\pi k^2 \varepsilon_w^2} \frac{e^{-kz}}{r^3}. \tag{12}$$

Please note that solving the Poisson-Boltzmann equation without considering the Debye-Huckel approximation for a distributed charge on a particle gives the same asymptotic solution than eq.12 rescaled with an effective charge [24]. In our case, from the numerical results of [24], we can estimate an effective charge smaller than 2×10^{-3} (for $R = 5\mu m$) and 2×10^{-2} (for $R = 200\mu m$) with respect to the real charge on the particle. Such small values of the effective charge support an even smaller effect of the electrostatic on the interface distortion. Taking into account the expression of $\wp(r)$ (Eq. 11), we can explicitly give the perturbation parameters $\epsilon_\wp$ and ϵ_F as:

$$\epsilon_\wp = \frac{\sigma_e^2}{2\gamma\varepsilon_w^2 k^2 \sin^5\theta R} \tag{13}$$

and

$$\epsilon_F = \epsilon_\wp + \frac{2\rho_p g f(\theta) R^2}{3\gamma \sin\theta}. \tag{14}$$

From Eq. 13, interface deformation due to electrodipping becomes more important when the particle size is smaller. Inversely the force on the particle is dominated by gravity for particle's radius larger than a critical radius R_C given by : $R_C = \sqrt[3]{3\sigma_e^2/4\varepsilon_w^2 k^2 \sin^4\theta g \rho_p f(\theta)}$. Taking typical material parameters as: $\varepsilon_w = 78$, $\gamma = 73 \times 10^{-3}$ N/m (resulting in a capillary length $\ell_C = 2.7$mm), a surface charge density on the particle $\sigma_e = 0.3e^-/\text{nm}^2$, $\rho_p = 1.055 \times 10^3$ kg m^{-3} (density of typical polystyrene particles), a Debye length $k^{-1} = 960$ nm and a contact angle $\theta = 60°$, the critical radius results in $R_C = 60$ nm. Such a small value ($R_C \ll k^{-1}$) should be taken with caution as it is beyond the validity limit of the model.

We are now able to evaluate the interface deformation h provoked by the presence of the particle and the force F acting on the particle. In Figure 3(a) is reported the interface profile for polystyrene beads of fixed contact angle $\theta = 60°$ and different radii ranging from $R = 5\mu$m to $R = 200\mu$m. For $R > 200\mu$m, the parameter $\epsilon_F > 0.033$ and we leave the limit of validity of the model, i.e. small interface deformation. In Figure 3(b) is shown the interface profile for a particle with fixed radius $R = 5\mu$m and different contact angles spanning a large range from 5° to 175°. All interface deformations relaxe over the capillary length. The interface deformation is sub-nanometric for particles with 5μm radius. The deformation amplitude reaches micro-metric values for particles of radius larger than 100μm. For a 5μm radius particle the dependence of the interface deformation over the particle contact angle is less than 10%.

In Figures 4(a) and 4(b) are reported the dependence of the amplitude of the interface deformation h with the particle radius R at fixed contact angle $\theta = 60°$ and with the particle contact angle θ at fixed radius $R = 5\mu$m,

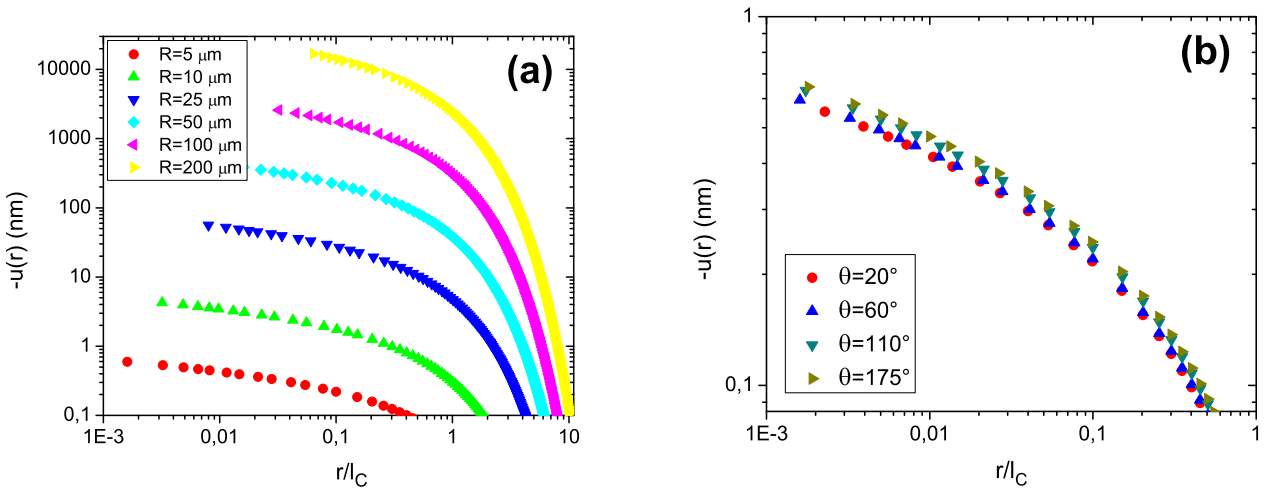

FIG. 3: Interface profile around polystyrene beads trapped at an air-water interface. (a) Different particle's radius with fixed contact angle $\theta = 60°$. (b) Different particle's contact angle with same radius $R = 5\mu$m.

respectively. At fixed contact angle, h is a monotonically increasing function of the particle size, having its maximum for the heaviest particle considered. The deformation amplitude for $R = 5\mu$m particles is not monotonic with θ showing a minimum at $\theta \approx 60°$. This behavior results from the opposite dependencies of gravity and electrostatic with the particle immersion depth. At small θ the particle is more immersed in water: gravity force is reduced by buoyancy while electrostatic pressure is enhanced by ions dissociation in water. At the opposite for larger θ the particle is more in air: gravity force is stronger and electrostatic pressure is weaker. A combination of the two opposite effects results in a minimum of the interface deformation at some intermediate angles.

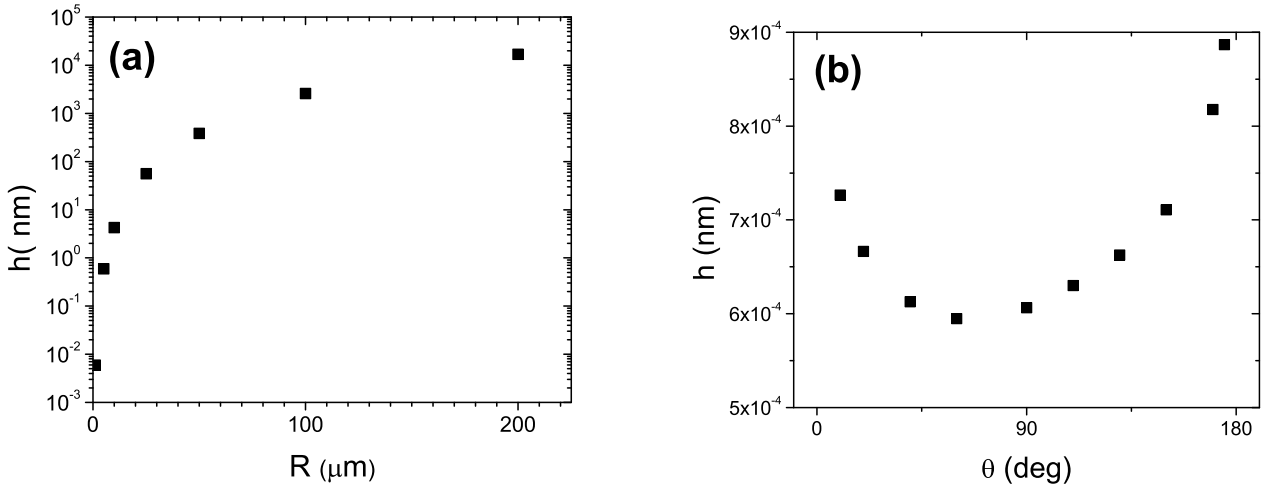

FIG. 4: Amplitude of the interface deformation h versus (a) the particle's radius for a fixed $\theta = 60°$ and (b) the particle's contact angle for a fixed $R = 5\mu$m.

The effective contact θ_{eff} angle is always lower than θ. In Figures 5(a) is shown the dependence of θ_{eff} with the particle radius R. The effective contact angle depends slightly on R. For a fixed contact angle of $\theta = 60°$, the lower effective contact angle results in $\theta_{eff} = 52.1°$ for the heaviest particle of $R = 200\mu$m. At fixed radius $R = 5\mu$m, the

contact angle deviation from θ is minimum at $\theta = 90°$ and slightly increases of $0.1°$ at low and high contact angles.

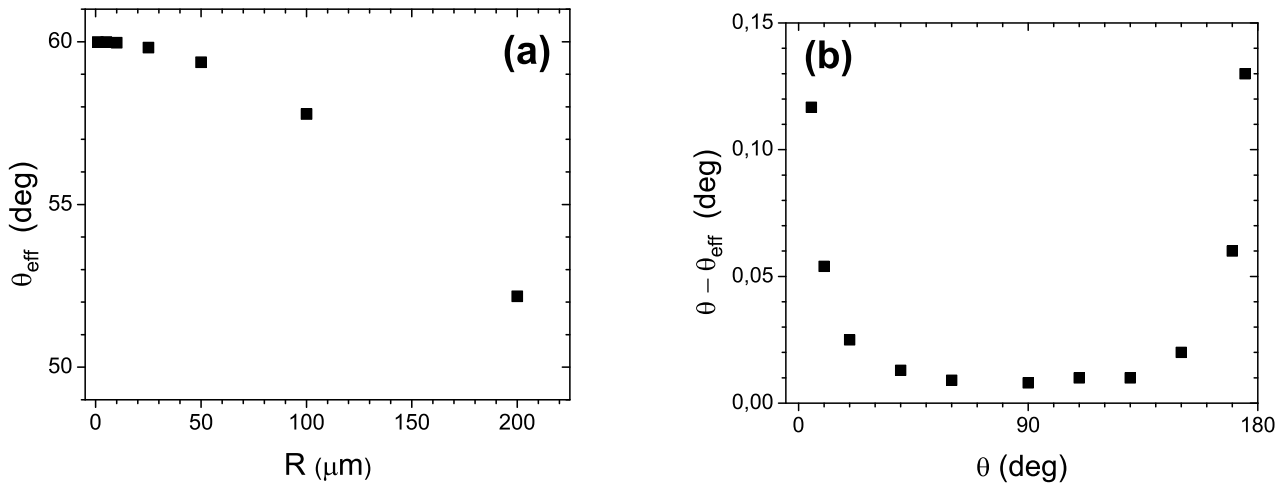

FIG. 5: Effective contact angle θ_{eff} versus (a) the particle radius for $\theta = 60°$ and (b) the contact angle for $R = 5\mu$m.

Finding the drag for a particle moving on a deformed interface is a very complex problem. It has been only recently tackled with a numerical approach [25] in the case of a cylinder (2D version of the problem). The influence of an important number of parameters such as the fluids and particle densities, the fluids viscosities and the particle contact angle on the particle drag has been evaluated. Unfortunately, both the geometry and considered values of particle size and density which contribute to the interface deformation do not match our values (corresponding to former experiments) preventing a quantitative comparison with our experimental results. These simulations nevertheless show that in the range of explored parameters the interface deformations contribution to the particle drag remains lower than 10%, which would indicate that the apparent contact angle is more relevant that the real one. Taking into account such difficulties, we use the Fisher model [19] by replacing the contact angle with the effective one in order to predict the effect of the interface deformation on the particle drag. Using this approximation we slightly overestimate the effect of the interface deformation on the particle drag as we replace the small volume of the air wedge with low viscosity close to the particle with an equivalent volume of water with larger viscosity. In Figure 6(a) is shown the ratio Γ_S/Γ_B versus the particle radius for a fixed contact angle of $\theta = 60°$. In absence of gravity and electrodipping such a ratio is independent from the radius. In our case it decreases slightly with the radius. In Figure 6(b) is reported the dependence of the ratio between the difference of surface diffusion coefficients and the bulk one $(D_S(\theta) - D_S(\theta_{eff})/D_B$ versus the contact angle for a particle of $R = 5\mu$m. This difference increases with the contact angle when the effect of gravity increases. It also slightly increases at very low angle due to the electrodipping effect.

In conclusion the signature of the interface deformation due to gravity on the particle diffusion is the predicted dependence of the diffusion coefficients ratio D_S/D_B versus the particle radius. For purely hydrodynamics theories[19, 20] and even for particle dynamics models including triple line dynamics[21] such a ratio is expected to be independent from the particle radius. Unfortunately for typical microparticle's mass and surface charge densities, the effect of gravity and electrostatic gives sub-nanometric interface deformations. Consequently the effect on the particle dynamics i.e. on the particle diffusion coefficient remains negligible. In our model, gravity starts to affect diffusion coefficient at the interface for particle radii above few ten of microns: the largest contribution is of the order of 3% for a particle of $R = 200\mu$m radius. Note that the model used here has been developed under the assumption of a point-like particle. Such an assumption implies that all the calculated quantities, like the electrostatic pressure on the surface, are strictly valid at distances much larger than the particle radius and the Debye length. The model also assumes that both water and air are dielectrics and that the air-water interface in presence of a charged particle has not a constant electrical potential. This hypothesis has to be taken with caution as some studies evidenced a negative equipotential air-water interface even in presence of charged particles. The surface potential may also affect the particle diffusion coefficient depending on the sign of particle charge[26]. We believe that the predicted influence of gravity on the particle diffusion or drag will stimulated new experiments in this field.

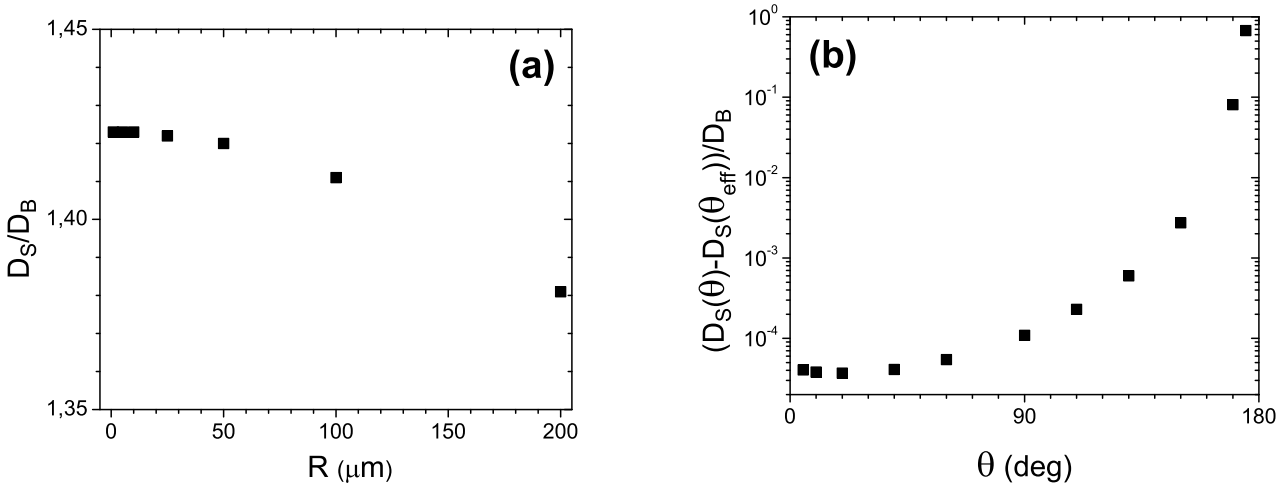

FIG. 6: (a) Surface over bulk diffusion coefficient ratio versus particle radius at fixed contact angle of $\theta = 60°$, (b) Normalized difference of the surface diffusion coefficient at contact angle θ and θ_{eff} versus the contact angle for a fixed radius of $R = 5\mu$m.

We gratefully acknowledge the financial support of ANR Surfanicol (ANR14-CE07-0039-01).

[1] C. Wei and T. Penger, Europhysics Letters **84**, 28003 (2008).
[2] R. Aveyard, B. P. Binks, and J. H. Clint, Adv. Colloid Interface Sciences **100-102**, 503 (2003).
[3] O. D. Velev, K. Furusawa, and K. Nagayama, Langmuir **12**, 2374 (1996).
[4] A. Dinsmore, M. F. Hsu, M. G. Nikolaides, M. Marquez, A. R. Bausch, and D. A. Weitz, Science **298**, 1006 (2002).
[5] P. Kralchevsky and N. D. Denkov, Current. Opinion Colloid Interface Science **6**, 383 (2001).
[6] P. A. Kralchevsky and K. Nagayama, livre (2011).
[7] F. Fan and K. J. Stebe, Langmuir **20**, 3062 (2004).
[8] M. Abkarian, J. Nunes, and H. A. J. Stone, American. Chemical. Society **126**, 5978 (2004).
[9] F. H. Martin, Advancement Materials **27**, 7065 (2015).
[10] P. Wongkongkatep, K. Manopwisedjaroen, P. Tiposoth, S. Archakunakorn, T. Pongtharangkul, M. Suphantharika, K. Honda, I. Hamachi, and J. Wongkongkatep, Langmuir **28**, 5729 (2012).
[11] P. Bernard, Current Opinion in Colloid and Interface Science **7**, 21 (2002).
[12] R. Aveyard, B. Binks, J. H. Clint, P. D. I. Fletcher, T. S. Horozov, B. Neumann, V. N. Paunov, J. Annesley, S. W. Botchway, D. Nees, et al., Physical Review Letters **88 (24)**, 246102 (2002).
[13] D. Vella and L. Mahadevan, American Journal of Physics **73**, 817 (2005).
[14] W. A. Ducker, Z. Xu, and J. Israelachvili, Langmuir **10**, 3279 (1994).
[15] M. G. Nikolaides, A. R. Bausch, M. F. Hsu, A. D. Dinsmore, M. P. Brenner, C. Gay, and D. A. Weitz, Nature (London) **420**, 299 (2002).
[16] M. Oettel, A. Dominguez, and S. Dietrich, Physical Review E **71**, 051401 (2005).
[17] M. Oettel and S. Dietrich, Langmuir **24**, 1425 (2008).
[18] L. Bai, J. Fruehwirth, X. Cheng, and W. Macosko, Soft Matter **11**, 5282 (2015).
[19] T. Fisher, P. Dhar, and P. Heinig, Journal of Fluid Mechanics **558**, 451 (2006).
[20] C. Pozrikidis, Journal of Fluid Mechanics **575**, 333 (2007).
[21] G. Boniello, C. Blanc, D. Fedorenko, M. Medfai, N. Mbarek, M. In, M. Gross, A. Stocco, and M. Nobili, Nature Materials **14**, 908 (2015).
[22] K. Danov, R. Aust, F. Durst, and U. Lange, Journal of Colloid and Interface Science **172**, 147 (1995).
[23] L. Foret and A. Wurger, Physical Review Letters **92**, 1 (2004).
[24] D. Frydel, S. Dietrich, and M. Oettel, Phys. Rev. Lett. **99**, 118302 (2007).
[25] J.-C. Loudet, M. Qiu, J. Hemauer, and J. Feng, Eur. Phys. J. E **43**, 13 (2020).
[26] T. Gehring and T. M. Fischer, The Journal of Physical Chemistry C **115**, 23677 (2011).